A new method of NMO and stacking for converted-wave processing

John J. Zhang

ABSTRACT

The traveltime curves of *P-S* reflections are not hyperbolic. Thus, the classical hyperbolic approximation may not be valid for converted-wave data processing. This paper presents a new method, which expands the t^2 -x^2 formula with only two terms because a higher-order Taylor series expansion is mathematically complicated and also becomes inaccurate with increasing offset. The coefficient of the second term can be calculated accurately through explicit equations. The second term can be also factorized into a squared constant and a squared variable, which amounts to a transformation of velocity and offset. In the transformed system, the traveltime curves are hyperbolic and conventional processing procedures can be carried out. Synthetic stacks indicate that this method is valid until the percentage error of v_p estimation is out of the range of –5% to 10%.

TWO-TERM TAYLOR-SERIES EXPANSION OF T^2 –X^2 CURVES

The travel time curve of a *P-P* or *S-S* reflection from a horizontal reflector below a homogeneous isotropic layer is a hyperbola in the *t-x* domain:

$$t^2 = t_0^2 + \frac{x^2}{v^2}, \tag{1}$$

where t is the travel time from the source to reflector and back to the receiver, x is the source-receiver distance, i.e., offset, t_0 is the travel time at zero offset, and v is the velocity. Equation (1) is a straight line if t^2 is viewed as the function of x^2. The t^2– x^2 curves from seismic data are routinely fitted linearly to give the intercept and the slope, which are interpreted as t_0^2 and $1/v^2$, respectively. For *P-S* reflections, the *t-x* relationship cannot be expressed in the same form as equation (1), but t^2 can still be seen as a function of x^2 (Copsen 1935; Taner and Koehler, 1969), i.e., $t^2 = f(x^2)$, which can be expanded in Taylor series about x^2=0:

$$t^2 = f(x^2) = f(0) + f'(0)x^2 + \frac{1}{2}f''(0)x^4 + \cdots\cdots. \tag{2}$$

Determination of the high-order derivatives starting from the third term in equation (2) is quite mathematically involved (Tessmer and Behle, 1988; Thomsen, 1999; Tsvankin and Thomsen, 1994). The attempt to approximate t^2 with more terms is not computationally efficient, and the approximations also become inaccurate with increasing offset because of truncation errors.

In fact, t^2 can be expressed as the sum of only two terms according to the Taylor series theorem. Equation (2) can be reformulated as:

$$t^2 = f(0) + f'(c)x^2 \\ = t_0^{\,2} + f'(c)x^2 \tag{3}$$

where $f(0)$ is t_0^2, f' is $d(t^2)/d(x^2)$ and c is some value between 0 and x^2. The terms c and $f'(c)$ are x dependent and equation (3) is not hyperbolic. On the other hand, $f'(x^2)$ can be defined as:

$$f'(x^2) = \frac{d(t^2)}{d(x^2)}$$

i.e,

$$d(t^2) = f'(x^2)dx^2 \tag{4}$$

Integrating both sides of equation (4) leads to:

$$\int_{t_0^2}^{t^2} d(t^2) = \int_0^{x^2} f'(x^2)d(x^2)$$

i.e.,

$$t^2 = t_0^2 + 2\int_0^x xf'(x^2)dx \tag{5}$$

A comparison of equation (3) with equation (5) results in:

$$f'(c) = (2\int_0^x xf'(x^2)dx)/x^2 . \tag{6}$$

It is noted from Figure 1 that the travel times and offsets for *P-S* reflections are related as:

$$x = v_{px}t_p + v_{sx}t_s \tag{7}$$

where v_{px}, t_p, v_{sx}, t_s are the horizontal components of velocity and traveltimes for *P* and *S* waves, respectively. As a result, $f'(x^2)$ can be derived as follows (Tsvankin and Thomsen, 1994):

$$f'(x^2) = \frac{d(t^2)}{d(x^2)} = \frac{t}{x}\frac{dt}{dx} = \frac{tp}{x} = \frac{t_p + t_s}{\frac{v_{px}}{p}t_p + \frac{v_{sx}}{p}t_s} \\ = \frac{1}{v_p^{\,2} + v_s^{\,2}\; t_s/t_p} + \frac{1}{v_s^{\,2} + v_p^{\,2} t_p/t_s} \tag{8}$$

where p is the ray parameter. The evaluation of f' reduces to the evaluation of t_s/t_p or t_p/t_s. The traveltime ratio t_p/t_s depends on the v_p/v_s ratio and offset/depth ratio (x/h). Let $x/h=\alpha$, $t_p/t_s=\beta$ and $v_p/v_s=\gamma$. They are related in the following formula (see APPENDIX A for derivation):

$$\beta^4 + \beta^3(2/\gamma^2) + \beta^2(\alpha^2 + 1 - \alpha^2\gamma^2 - \gamma^2)/\gamma^4 + \beta(-2/\gamma^4) - 1/\gamma^6 = 0 \qquad (9)$$

The t_p/t_s (β) can be solved from equation (9) as a function of x/h (α) and v_p/v_s (γ). Beyer (1984) gives a detailed analytical solution (see APPENDIX B for details). For a given geological model, v_p, v_s, v_p/v_s and h are fixed and $f^{'}$ is a function of offset x only.

In summary, $t^2 = f(x^2)$ for the *P-S* reflection can be expressed as the sum of two-term Taylor series in equation (3), and $f^{'}(c)$ in this formula can be computed through equations (6), (8) and (9).

NMO AND STACKING FOR SYNTHETIC DATA

As stated in equation (3), $f^{'}(c)$ is offset-dependent. Direct t^2–x^2 curve-fitting for NMO calculation and stacking may be of poor quality, especially at far offsets. In order to make the traveltime curves hyperbolic, the original offsets have to be adjusted. The scheme for offset modification as shown in Figure 1 is to assume that a wave propagates at constant velocity from a new source X_{Snew} to the *CCP* and then reflects back to a new receiver X_{rnew}, and that the time it takes is equal to that for the *P-S* reflection time. According to this procedure the fabricated constant velocity is the harmonic average of v_p and v_s so that the travel times at zero offset are equal, which is expressed as:

$$\frac{1}{V} = \frac{1}{2}\left(\frac{1}{v_p} + \frac{1}{v_s}\right) \qquad (10)$$

The adjusted offsets are computed as follows:

$$t_0^2 + f^{'}(c)x^2 = t_0^2 + \frac{X^2}{V^2} \Rightarrow \quad X = \sqrt{f^{'}(c)x^2V^2} \qquad (11)$$

where V is the fabricated velocity, X is the new offset and x is the original offset. The manipulation in equations (10) and (11) amounts to factorizing the second term, $f^{'}(c)\, x^2$ in equation (3), into a squared new offset variable multiplied by a squared new constant. As indicated in equations (12) and (13), the new velocity and new offsets create hyperbolic travel time curves. Standard NMO, stacking and other processing procedures can be then carried out.

$$t^2 = t_0^2 + \frac{X^2}{V^2} \qquad (12)$$

$$NMO = t - t_0 = t - \sqrt{t^2 - \frac{X^2}{V^2}} = t\left(1 - \sqrt{1 - \frac{X^2}{t^2V^2}}\ \right). \qquad (13)$$

Figure 2 on the right shows the hyperbolic fitting to the original *t-x* curve for a reflector buried at 1500 m. The *t-x* curve is not hyperbolic and NMO calculation is inaccurate based on this hyperbolic fitting. Consequently, the stacked section on the left side of Figure 2 has smaller peak amplitude and poor resolution. For example, there are two separate small peaks generated from one reflector. Figure 3 on the right is the hyperbolic fitting to the transformed *t-X* curve. The shortened offsets due to transformation can be observed. The t–X curve is hyperbolic and the NMO calculation is accurate. Figure 3 shows large peak amplitude and high resolution to the left.

SYNTHETIC RESULTS BASED ON VELOCITY ESTIMATES

The above transformation of velocity and offsets requires a knowledge of depth and velocities, which, in reality, are estimated from seismic data. For a simple case shown in Figure 1, v_p can be evaluated from stacking velocity on *P-P* sections. The stacking velocity obtained from *P-S* sections may approximately represent the arithmetic average of v_p and v_s. As a result, v_s can be derived. Moreover the depth h can be computed from v_p, v_s, and t_0, which is acquired from hyperbolic fitting to the original t-x curve for the *P-S* reflection. The errors in the process of estimation may be large and the method may not be very useful. In order to test the validity, the exact value and inaccurate values of v_p are substituted into this procedure for computation of v_s and h. With the availability of v_p, v_s, and h, the new adjusted offsets can be calculated based on equation (11) and then equations (6), (8) and (9). The conclusions regarding the sensitivity of the results to the errors of velocity and depth can then be drawn from a comparison of stacked seismic sections.

In Figure 4, the transformed offsets were calculated based on the estimates of velocities and depth. v_p is precise, v_s has the positive percentage error of 8.5% and h is 15% greater than the exact value. Hyperbolic fitting to the t-X curve was performed for NMO calculation and stacking. As shown on the left of Figure 4, the stacking results are close to those in Figure 3 in terms of peak amplitude and resolution. Compared with Figure 2, it is significantly improved with much higher peak amplitude and better resolution.

Adding 10% positive percentage error to v_p results in -11.5% percentage error in v_s and -3.8% percentage error in depth, in accordance with the process of estimation. The inaccurate velocities and depth were then input for calculation of new transformed offsets. Similarly NMO calculation and then stacking were conducted based on hyperbolic fitting to t-X curve. As shown in Figure 5, the peak amplitude is smaller than in Figure 3, but it is still bigger than in Figure 2. Most importantly, the resolution is enhanced appreciably. Given –5% percentage error in v_p, 18.5% percentage error in v_s and 11.2% percentage error in depth result. As shown in Figure 6, the results are close to those in Figure 5 in terms of peak amplitude and resolution.

In Figure 7, the percentage error in v_p is out of the range of –5% to10%. Consequently, the generated synthetic sections are not better than in Figure 2. In other words, the method will become invalid when errors are considerable.

CONCLUSIONS

The *P-S* traveltime curves for converted waves are not hyperbolic, but t^2–x^2 can be expanded in a Taylor series about x^2 =0 with only two terms. The coefficient of the second term, which is offset dependent, can be calculated accurately using an explicit expression. The second term can also be factorized into a squared constant and a squared variable, which is equivalent to the transformation of velocity and offset into a new system. In this system, the traveltime curves are hyperbolic so that standard processing procedures can be used with good results. Synthetic seismic data indicate that the method improves NMO and stacking quality considerably as long as the percentage error in v_p is within –5% to 10%. v_p out of this range causes degradation in the results.

REFERENCES

Beyer, W. H., 1984, Standard mathematical tables, Boca Raton: CRC Press, Inc.

Copson, C. T., 1935, Theory of functions of a complex variable, Oxford: Oxford Universiy Press.

Taner, M. T., and Koehler, F., 1969, Velocity spectra-digital computer derivation and applications of velocity functions, Geophysics, **34**(6), 859-881.

Tessmer, G., and Behle, A., 1988, Common reflection point data-stacking technique for converted waves, Geophysical Prospecting, **6**, 671-688.

Thomsen, L., 1999, Converted-wave reflection seismology over inhomogeneous, anisotropic media, Geophysics, **64**(3), 678-690.

Tsvankin, L., and Thomsen L., 1994, Nonhyperbolic reflection moveout in anisotropic media, Geophysics, **59**(8), 1290-1304.

ACKNOWLEDGMENTS

I would like to express my appreciation to the CREWES sponsors for their support of this research. I am also indebted to Chuck Ursenbach, Pat Daley and Larry Lines for their critical reviews and helpful suggestions. Finally I extend my sincere thanks to Rob Stewart, Gary Margrave, Don Lawton, Larry Lines and Jim Brown, who taught me advanced knowledge in seismic converted-wave exploration.

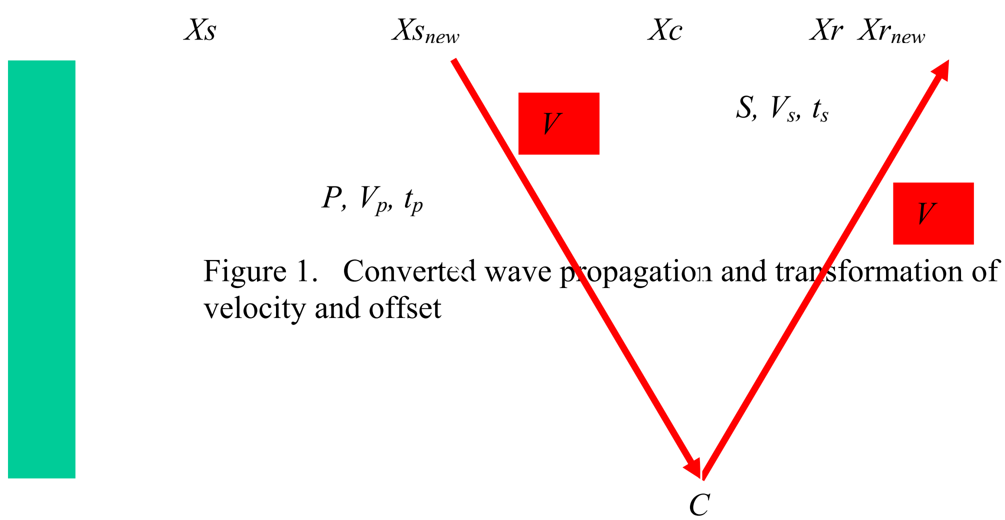

FIG. 1. Converted wave propagation and transformation of velocity and offset

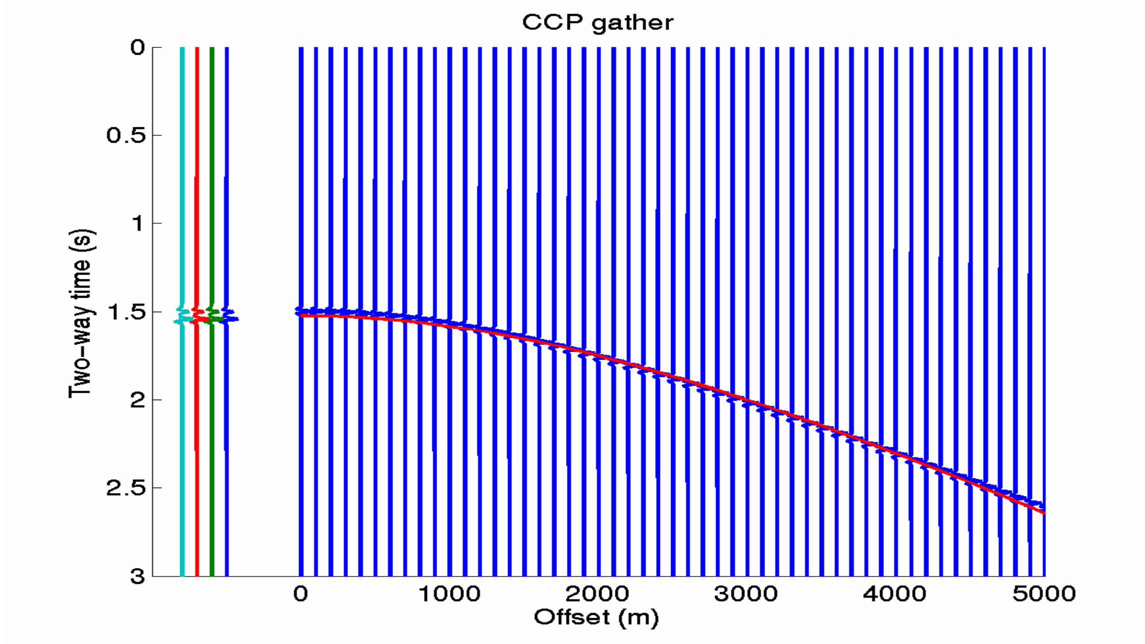

FIG. 2. Hyperbolic fitting and stacking using conventional processing procedures for a *CCP* gather (v_p*=3000m/s,* v_s*=1500m/s* and *h=1500m*). The red line is the hyperbolic curve fitted to the data for NMO and stacking. As shown on stack sections, two small peak amplitudes are generated from one reflector.

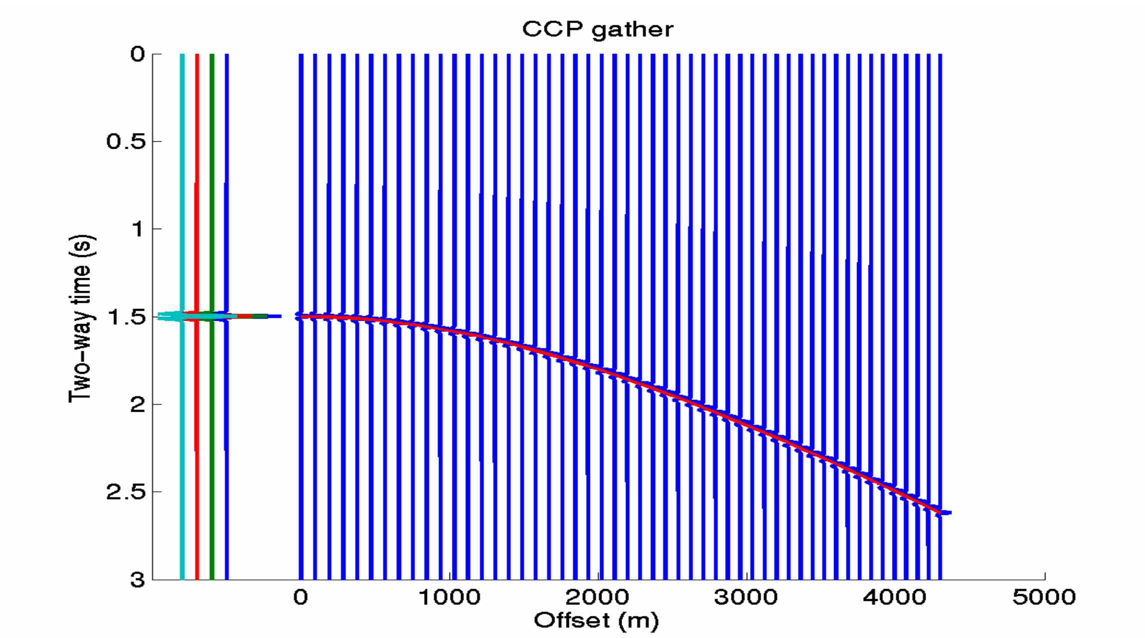

FIG. 3. Hyperbolic fitting and stacking using conventional processing procedures for a *CCP* gather with transformed offsets calculated from the accurate velocities and depth (v_p*=3000m/s,* v_s*=1500m/s,* and *h=1500m*). The red line is the hyperbolic curve fitted to the data for NMO and stacking. As shown on stack sections, there is only one large peak amplitude from one reflector.

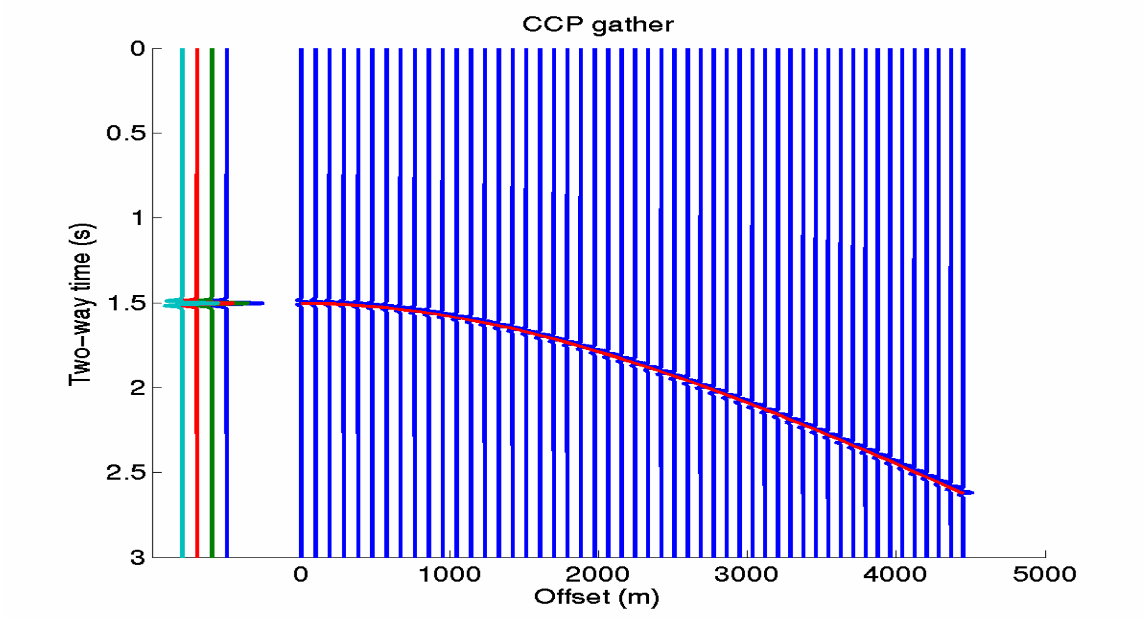

FIG. 4. Hyperbolic fitting and stacking using conventional processing procedures for a *CCP* gather with transformed offsets calculated from the estimated velocities and depth (v_p=3000m/s, v_s=1500m/s+8.5%×1500m/s, and *h*=1500m+7.2%×1500m). The red line is the hyperbolic curve fitted to the data for NMO and stacking. As shown on stacked sections, the peak amplitude is smaller than that in Figure 3, but it is still much bigger than that in Figure 2 and the resolution is also much improved relative to Figure 2.

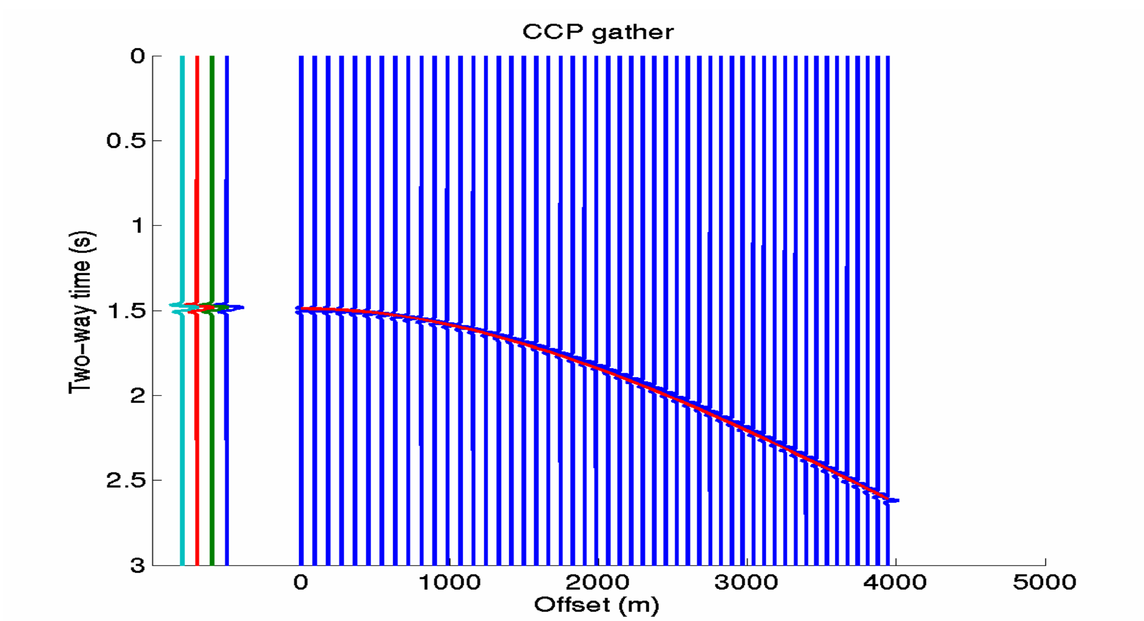

FIG. 5. Hyperbolic fitting and stacking using conventional processing procedures for a *CCP* gather with transformed offsets calculated from the estimated velocities and depth (v_p=3000m/s+10%×3000m/s, v_s=1500m/s−11.5%×1500m/s, and *h*=1500m−3.8%×1500m). The red line is the hyperbolic curve fitted to the data for NMO and stacking. As shown on stacked sections, the peak amplitude is smaller than that in Figure 4, but it is still bigger than that in Figure 2 and the resolution is also better than that in Figure 2.

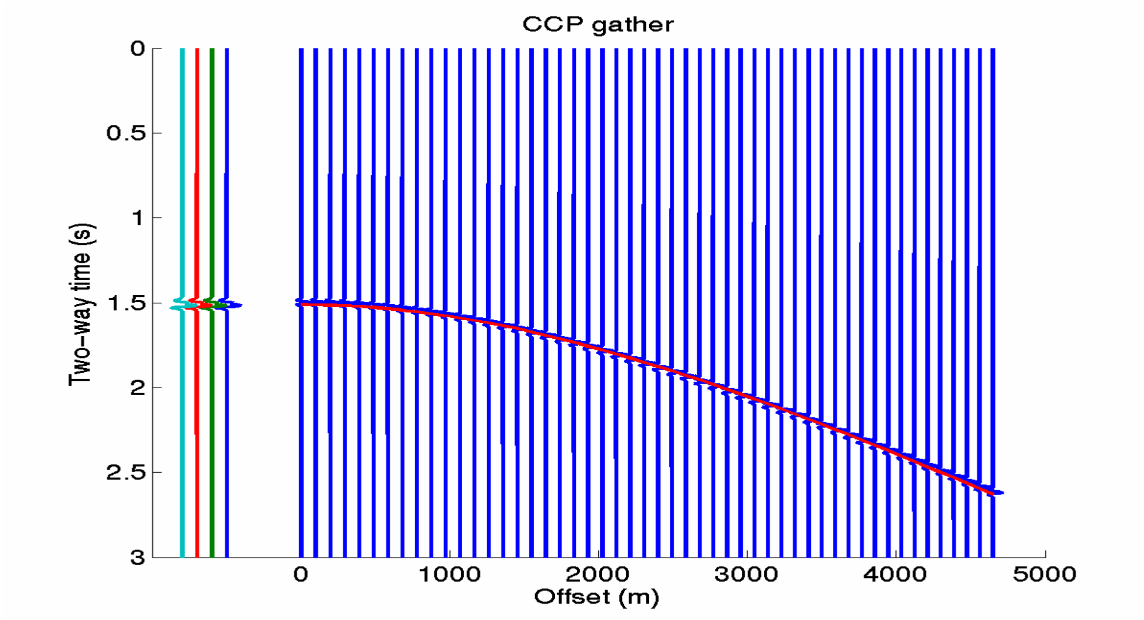

FIG. 6. Hyperbolic fitting and stacking using conventional processing procedures for a *CCP* gather with transformed offsets calculated from the estimated velocities and depth (v_p=3000m/s−5%×3000m/s, v_s=1500m/s+18.5%×1500m/s, and *h*=1500m+11.2%×1500m). The red line is the hyperbolic curve fitted to the data for NMO and stacking. As shown on stacked sections, the peak amplitude is smaller than that in Figure 4, but it is a little bigger than that in Figure 2 and the resolution is also better than that in Figure 2.

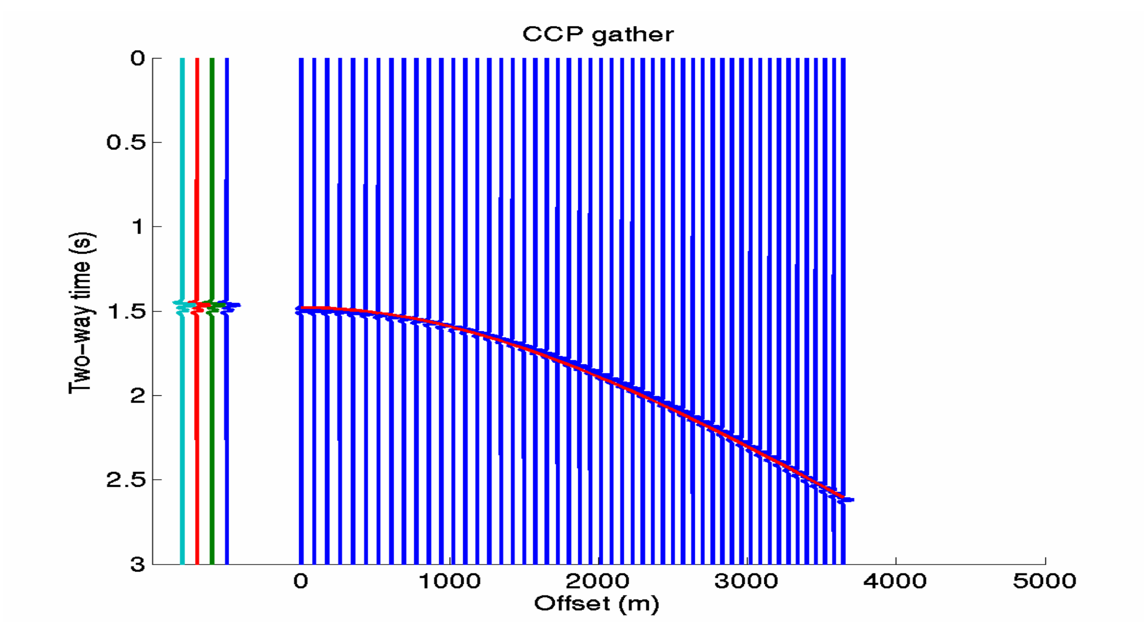

FIG. 7. Hyperbolic fitting and stacking using conventional processing procedures for a *CCP* gather with transformed offsets calculated from the estimated velocities and depth (v_p=3000m/s+15%×3000m/s, v_s=1500m/s−21.5%×1500m/s, and *h*=1500m−10.8%×1500m). The red line is the hyperbolic curve fitted to the data for NMO and stacking. As shown on stacked sections, the results are degraded with no higher peak amplitude and better resolution than in Figure 2.

APPENDIX A

As shown in Figure 1, $t_p = X_sC/V_p$ and $t_s = CX_r/V_s$, i.e.,

$$\begin{aligned}(\frac{t_p}{t_s})^2 &= (\frac{X_sC/v_p}{CX_r/v_s})^2 \\ &= (\frac{X_sC}{CX_r})^2(\frac{v_s}{v_p})^2 \\ &= \frac{X_sX_c^2 + X_cC^2}{(X_sX_r - X_sX_c)^2 + X_cC^2}(\frac{v_s}{v_p})^2\end{aligned} \tag{A1}$$

Note:

$$\begin{aligned}X_sX_c &= v_pt_p\sin\theta \\ &= v_p^2t_pp\end{aligned} \tag{A2}$$

$$X_cX_r = v_s^2t_sp \tag{A3}$$

where θ is the incident angle and p is the ray parameter. It can be derived from equations (A2) and (A3):

$$\frac{X_sX_c}{X_sX_r} = \frac{X_sX_c}{X_sX_c + X_cX_r} = \frac{v_p^2t_pp}{v_p^2t_pp + v_s^2t_sp} = \frac{1}{1 + \frac{1}{(v_p/v_s)^2(t_p/t_s)}}$$

i.e.,

$$X_sX_c == \frac{X_sX_r}{1 + \frac{1}{(v_p/v_s)^2(t_p/t_s)}} \tag{A4}$$

Let $x = X_sX_r$, $h = X_cC$, $\alpha = x/h$, $\beta = t_p/t_s$ *and* $\gamma = v_p/v_s$. Substituting equation (A4) into equation (A1) results in:

$$\beta^2 = \frac{(\frac{x}{1+\frac{1}{\gamma^2\beta}})^2 + h^2}{(x - \frac{x}{1+\frac{1}{\gamma^2\beta}})^2 + h^2}\,\frac{1}{\gamma^2}$$

$$= \frac{(\frac{\alpha}{1+\frac{1}{\gamma^2\beta}})^2 + 1}{(\alpha - \frac{\alpha}{1+\frac{1}{\gamma^2\beta}})^2 + 1} \frac{1}{\gamma^2}$$

$$= \frac{(\frac{\alpha\beta\gamma^2}{\gamma^2\beta+1})^2 + 1}{(\alpha - \frac{\alpha\beta\gamma^2}{\gamma^2\beta+1})^2 + 1} \frac{1}{\gamma^2}$$

$$= \frac{(\alpha\beta\gamma^2)^2 + (\gamma^2\beta+1)^2}{[\alpha(\gamma^2\beta+1) - \alpha\beta\gamma^2]^2 + (\gamma^2\beta+1)^2} \frac{1}{\gamma^2}$$

i.e.,

$$\beta^2\gamma^2[\alpha^2 + (\gamma^2\beta+1)^2] = (\alpha\beta\gamma^2)^2 + (\gamma^2\beta+1)^2 \qquad \text{(A5)}$$

Reorganizing equation (A5) leads to:

$$\beta^4 + \beta^3(2/\gamma^2) + \beta^2(\alpha^2 + 1 - \alpha^2\gamma^2 - \gamma^2)/\gamma^4 + \beta(-2/\gamma^4) - 1/\gamma^6 = 0 \qquad \text{(A6)}$$

APPENDIX B

A quartic equation has the form (Beyer, 1984):

$$x^4 + ax^3 + bx^2 + cx + d = 0 \qquad \text{(B1)}$$

which has the resolvent cubic equation:

$$y^3 - by^2 + (ac - 4d)y - a^2d + 4bd - c^2 = 0 \qquad \text{(B2)}$$

Equation (B2) has the analytical solution in APPENDIX C. Let y be any root of equation (B2), and

$$R = \sqrt{\frac{a^2}{4} - b + y} \qquad \text{(B3)}$$

If R is not equal to zero, then let

$$D = \sqrt{\frac{3a^2}{4} - R^2 - 2b + \frac{4ab - 8c - a^2}{4R}} \tag{B4}$$

$$E = \sqrt{\frac{3a^2}{4} - R^2 - 2b - \frac{4ab - 8c - a^2}{4R}} \tag{B5}$$

If R is equal to zero, then let

$$D = \sqrt{\frac{3a^2}{4} - 2b + 2\sqrt{y^2 - 4d}} \tag{B6}$$

$$E = \sqrt{\frac{3a^2}{4} - 2b - 2\sqrt{y^2 - 4d}} \tag{B7}$$

Then the four roots of equation (B1) are given by

$$x_1 = -\frac{a}{4} + \frac{R}{2} + \frac{D}{2} \qquad x_2 = -\frac{a}{4} + \frac{R}{2} - \frac{D}{2}$$

$$x_3 = -\frac{a}{4} - \frac{R}{2} + \frac{E}{2} \qquad x_4 = -\frac{a}{4} - \frac{R}{2} - \frac{E}{2}$$

APPENDIX C

A cubic equation has the form:

$$y^3 + py^2 + qy + r = 0 \tag{C1}$$

which may be reduced, by substituting for *y* the value *x-p/3*, to the following form (Beyer, 1984):

$$x^3 + ax + b = 0 \tag{C2}$$

where $a=1/3(3q-p^2)$ and $b=1/27(2p^3 - 9pq+27r)$.

Let

$$A = \sqrt[3]{-\frac{b}{2} + \sqrt{\frac{b^2}{4} + \frac{a^3}{27}}}, \qquad B = -\sqrt[3]{\frac{b}{2} + \sqrt{\frac{b^2}{4} + \frac{a^3}{27}}}$$

Then three roots of equation (C2) are given by:

$$x_1 = A + B,$$

$$x_2 = -\frac{A+B}{2} + \frac{A-B}{2}\sqrt{-3}$$

$$x_3 = -\frac{A+B}{2} - \frac{A-B}{2}\sqrt{-3}$$

Then three roots of equation (C1) are given by:

$$y_1 = A + B - \frac{p}{3},$$

$$y_2 = -\frac{A+B}{2} + \frac{A-B}{2}\sqrt{-3} - \frac{p}{3}$$

$$y_3 = -\frac{A+B}{2} - \frac{A-B}{2}\sqrt{-3} - \frac{p}{3}$$